Published in IET Microwaves, Antennas & Propagation
Received on 7th January 2010
Revised on 2nd July 2010
doi: 10.1049/iet-map.2010.0005

ISSN 1751-8725

2.4 GHz antenna array using vector modulator-based active phase shifters for beamforming

F. Hutu D. Cordeau J.-M. Paillot

Laboratoire d'Automatique et d'Informatique Industrielle, EA 1219, University of Poitiers, LAII, 4 av. de Varsovie, 16021 Angoulême Cedex, France
E-mail: david.cordeau@univ-poitiers.fr

Abstract: This study presents the analysis and the experimental results of a 2.4 GHz antenna array using vector modulators working as active phase shifters for beamforming. With the use of such an active phase shifter, a continuously controlled 360° phase shifting range can be achieved leading to an efficient beamforming architecture. To show the robustness of this system, a theoretical analysis is first performed in order to quantify the impact of vector modulators I/Q mismatch on the obtained gains and phase shifts. In the same way, the impact of the vector modulators noisy command voltages is also quantified by system simulations. The experimental results of the 2.4 GHz vector modulators show a maximum relative gain error close to 2.5% and an absolute phase error less than 3°. The measured 1 dB output compression point is −6 dBm. Measurements of the prototype including an array of four 'patch' antennas controlled by the vector modulators were also performed in an anechoic chamber. The results show good agreement between measured and theoretical radiation patterns.

1 Introduction

Beamforming systems are widely used in defense applications and civil radio communications [1–4]. Moreover, it is now well known that the use of a communication system having beamforming technology allows one to increase the spectral efficiency and to reduce the multi path fading, the bit-error rate and the co-channel interferences. This is commonly achieved by using directional antennas that provide high gain in the signal of interest direction and nulls in the interference signals directions. In order to obtain this property, the radio frequency (RF) signal must be applied to an antenna array with different phases and amplitudes.

Indeed, a beamforming system or a smart antenna [5–9] is generally made of an array of individual radiative elements (elementary antennas) that are placed in a particular configuration (linear, circular or matrix) as shown in Fig. 1. It is also made of an RF front-end which, among other functions, must change the amplitudes and phases of the signal associated to each elementary antenna. The RF front-end is driven by a digital signal processor that dynamically computes the amplitudes and phases values in order to maximise the performances of the communication system. By gathering the elementary antennas in such arrays and by changing the characteristics of the signals associated to each element, the array can present different gains according to the direction and, because of the property of reciprocity of the antennas, the radiation patterns are identical both on emission and reception.

Several solutions, with phase shifters or phase shifterless [10–13], are proposed to achieve this electronic modification of the radiation pattern. Indeed, passive phase shifters can be used to perform the phase control. Unfortunately their losses degrade the overall system performances. Other solutions such as Rotman lenses [14] or Butler matrices [15] can also be used especially for beam-steering and switched beam antenna arrays.

Concerning the phase-shifterless solutions, Ali Hajimiri and his work group recently proposed an architecture using a polyphase voltage-controlled oscillator, which is able to generate the local oscillator frequency with N phases. In this architecture, all the N phases are conveyed to each antenna via a distribution network. Phase selectors ensure the required phase to each element [11, 12]. In this case, the phase variations are discrete, which does not constitute

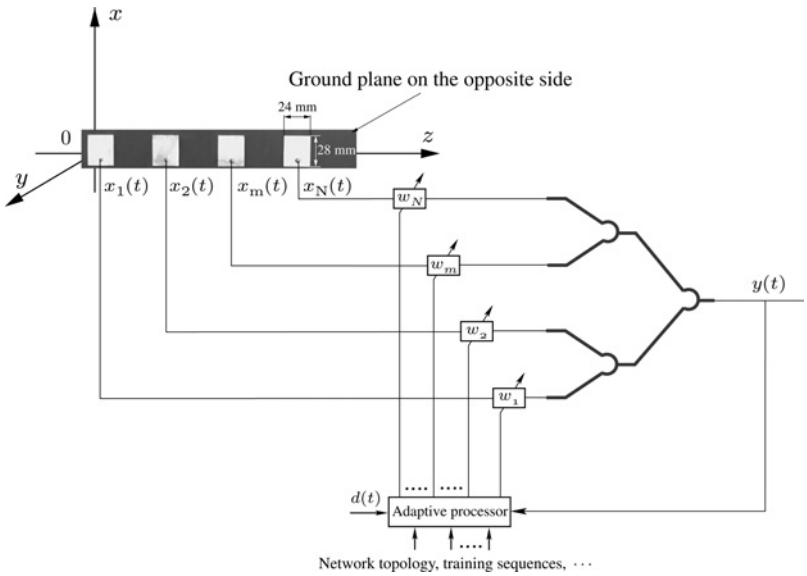

Figure 1 *Four 'patch' antennas in a beamforming configuration*

a problem as long as the discrimination steps are adequate to the application. Nevertheless, the distribution network of N phases constitutes a real issue here since each path must be forwarded to the phase selector in a symmetrical way.

On the other hand, an active solution presented by Lynch and York [10, 16, 17] uses a coupled oscillator array to control the relative phases through adjustment of oscillators' free-running frequencies. Moreover, recent works [18] present how the phase variation can be supplied by changing only the free-running frequencies of all coupled oscillators in the array. Despite the fact that a continuous phase variation can be obtained, this technique seems to be relatively complex to implement and the theoretical maximum relative phase is equal to $\pm 90^{\circ}$.

Other active solutions using vector modulators as phase shifters have been presented in [19–22], but none of these works presents the measurement results of the entire system including the antenna array. More recent works [23–25] present the realisation and radiation pattern measurements of a complete prototype that is able to perform beamforming by using a cooperative algorithm (particle swarm optimisation, PSO). This algorithm overcame the problem of various jammers positions placed both in the far-field and in the near-field from the antenna position. Moreover, the prototype is able to adapt radiation pattern in real-time scenarios. Nevertheless, the complexity of this prototype is relatively important since the radiating module and the hardware control module are not implemented on the same board. Furthermore, those works mainly deal with the adaptive behaviour of the prototype, but no design considerations concerning the impact of vector modulators I/Q mismatch on the radiation pattern and on the transmission quality are given.

In general, it is also possible to implement beamforming at the baseband stage with a digital approach. However, despite the fact that there is no need to use specific phase-shifting blocks, this solution leads to substantial complexity and high power consumption since the entire transmitter/receiver chain must be repeated several times.

On the other hand, the analogue beamforming in the RF path is more efficient since only the power amplifiers (PAs) and the phase shifters need to be repeated several times. This leads to the reduction of the size, weight and battery power consumption in the case of adaptive user terminals development for instance. Nevertheless, on the receiver side, one of the drawbacks of this architecture is that the baseband signal on all elements cannot be treated, but only the output represented by the sum of the weighted signals of individual antennas. Fortunately, adaptive algorithms are developed for this specific architecture: for example, gradient-based adaptive algorithms [26] and direction of arrival estimation by MUSIC-like algorithms [27].

Several other approaches, which are based on global optimisation tools such as the PSO algorithm [28–30], have been developed in the last years. By using this algorithm, there is no need to estimate the covariance matrix of the desired signal from the measurements of the received signal (as in least mean square (LMS) algorithms) which is computer costly.

In this context, the aim of this work is to present both design considerations and measurements of a 2.4 GHz antenna array using an architecture based on vector modulators. The 2.4 GHz frequency corresponds to the IEEE 802.11 b/g Wi-Fi standard. The presented prototype is able to modify the amplitudes and phases of the RF signals injected to patch antennas. This prototype is the first step to a complete one which will allow one to perform beamforming at the receiver.

doi: 10.1049/iet-map.2010.0005

The paper is organised as follows. In Section 2, the vector modulator-based active phase shifter architecture is studied. In particular, the influence of the vector modulator I/Q mismatch on the synthesised phases and amplitudes of the signals applied to each elementary antenna will be raised and the impact of noisy DC command voltages on the communication system performances will be studied. The experimental results of the prototype are presented in Section 3 and the paper is concluded in Section 4.

2 Vector modulator-based active phase shifter structure

2.1 Vector modulator I/Q mismatch

As mentioned previously, the architecture studied in this paper uses vector modulators as active phase shifters to achieve the required amplitudes and phases of the signals applied to each elementary antennas. Nevertheless, in a beamforming system, the precision of the radiation pattern depends on the accuracy of those synthesised amplitudes and phases.

Thus, in order to quantify the impact of vector modulators I/Q mismatch on the synthesised amplitudes and phases, let us consider a common vector modulator structure (Fig. 2).

If all the elements in this structure have an ideal behaviour, the gain of the active phase shifter is G_{th} and the synthesised phase shift is Φ_{th}. These values are obtained if V_{I} and V_{Q} DC voltages are the following [31]

$$\begin{cases} V_{\text{I}} = \dfrac{G_{\text{th}}}{\sqrt{2}}(\cos\Phi_{\text{th}} + \sin\Phi_{\text{th}}) \\ V_{\text{Q}} = \dfrac{G_{\text{th}}}{\sqrt{2}}(\cos\Phi_{\text{th}} - \sin\Phi_{\text{th}}) \end{cases} \tag{1}$$

Let us now define ε_A and ε_q the amplitude mismatch and the phase imbalance, respectively, in the I and Q paths of the active phase shifter. Then, the relative gain error $\varepsilon_{\text{rel},G}$ and the absolute phase error ε_Φ can be expressed as follows

$$\begin{cases} \varepsilon_{\text{rel},G} \triangleq \dfrac{G_N - G_{\text{th}}}{|G_{\text{th}}|} \cdot 100(\%) \\ \varepsilon_\Phi \triangleq |\Phi_N - \Phi_{\text{th}}|(\text{deg}) \end{cases} \tag{2}$$

where G_N and Φ_N are the obtained gains and phase shifts in the presence of mismatch.

Now, considering only the impact of an ε_A amplitude mismatch and according to Fig. 2, the output signal $S(t)$ of the vector modulator can be expressed as follows

$$\begin{aligned} S(t) = {} & (A - \varepsilon_A)\cos\left(\omega_0 t + \frac{\pi}{4}\right) \times \frac{G_{\text{th}}}{\sqrt{2}}(\cos\Phi_{\text{th}} + \sin\Phi_{\text{th}}) \\ & + (A + \varepsilon_A)\cos\left(\omega_0 t - \frac{\pi}{4}\right) \times \frac{G_{\text{th}}}{\sqrt{2}}(\cos\Phi_{\text{th}} - \sin\Phi_{\text{th}}) \end{aligned} \tag{3}$$

Thus, after calculation, the relative gain error $\varepsilon_{\text{rel},G}|_{\varepsilon_A}$ and the absolute phase error $\varepsilon_\Phi|_{\varepsilon_A}$ because of the ε_A amplitude mismatch can be written as

$$\begin{cases} \varepsilon_{\text{rel},G}|_{\varepsilon_A} = \left(-1 + \sqrt{1 + k_A{}^2 - 2k_A \sin 2\Phi_{\text{th}}}\right) \cdot 100(\%) \\ \varepsilon_\Phi|_{\varepsilon_A} = \left|\arctan\dfrac{-k_A \cos 2\Phi_{\text{th}}}{1 - k_A \sin 2\Phi_{\text{th}}}\right|(\text{deg}) \end{cases} \tag{4}$$

where $k_A = \varepsilon_A/A$ with A representing the amplitude at the filter output without mismatch.

In these conditions, Fig. 3*a* shows the relative gain error $\varepsilon_{\text{rel},G}$ and Fig. 3*b* the absolute phase error ε_Φ against k_A and imposed Φ_{th} phase shift. According to Fig. 3*a*, the absolute value of the relative gain error is maximum for an imposed phase shift Φ_{th} equal to $+45^\circ$ and -45° and for instance, an absolute value of the relative gain error less than 6% is obtained for k_A less than 0.06 irrespective of the imposed phase shifts $\Phi_{\text{th}} \in [-90^\circ \cdots 90^\circ]$. From Fig. 3*b*, it can be concluded that the absolute phase error is maximum when Φ_{th} equals 0°, -90° and $+90^\circ$. Furthermore, let us note that ε_Φ is equal to 0° when Φ_{th} equals $\pm 45^\circ$ irrespective of k_A. Moreover, one can note that an absolute phase error less than 3.3° is obtained for k_A less than 0.06 irrespective of the imposed phase shifts $\Phi_{\text{th}} \in [-90^\circ \cdots 90^\circ]$.

Let us now consider the impact of an ε_q phase imbalance and according to Fig. 2 again, the output signal $S(t)$ of the

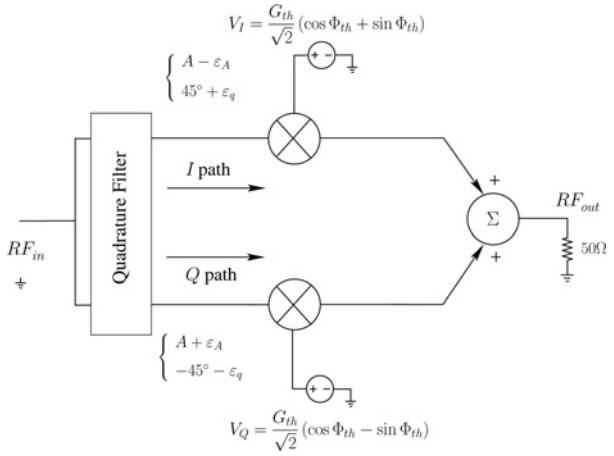

Figure 2 *Common vector modulator-based active phase shifter*

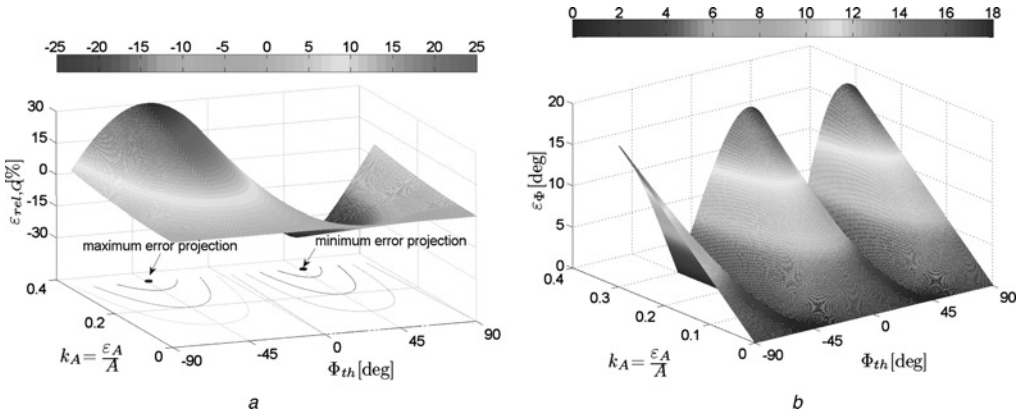

Figure 3 *Influence of the ε_A amplitude mismatch*

a Relative gain error $\varepsilon_{\text{rel},G}$
b Absolute phase shift error ε_Φ

vector modulator can be expressed as

$$S(t) = A\cos\left(\omega_0 t + \frac{\pi}{4} + \varepsilon_q\right) \times \frac{G_{\text{th}}}{\sqrt{2}}(\cos\Phi_{\text{th}} + \sin\Phi_{\text{th}}) + A\cos\left(\omega_0 t - \frac{\pi}{4} - \varepsilon_q\right) \times \frac{G_{\text{th}}}{\sqrt{2}}(\cos\Phi_{\text{th}} - \sin\Phi_{\text{th}}) \tag{5}$$

In the same way, the relative gain error $\varepsilon_{\text{rel},G}|_{\varepsilon_q}$ and the absolute phase error $\varepsilon_\Phi|_{\varepsilon_q}$ because of the ε_q quadrature mismatch can then be written as follows

$$\begin{cases} \varepsilon_{\text{rel},G}|_{\varepsilon_q} = \left(-1 + \sqrt{M^2 + N^2}\right) \cdot 100(\%) \\ \varepsilon_\Phi|_{\varepsilon_q} = \left|\arctan\dfrac{N}{M} - \Phi_{\text{th}}\right|(\text{deg}) \end{cases} \tag{6}$$

with

$$M = -\sqrt{2}\sin\left(\varepsilon_q - \frac{\pi}{4}\right)\cos\Phi_{\text{th}} \tag{7}$$

and

$$N = \sqrt{2}\cos\left(\varepsilon_q - \frac{\pi}{4}\right)\sin\Phi_{\text{th}} \tag{8}$$

Thus, using (6), Figs. 4*a* and *b* can be plotted. As shown in Fig. 4*a*, the absolute value of the relative gain error is maximum when Φ_{th} equals 0° and zero when Φ_{th} equals $\pm 45°$ irrespective of ε_q. Moreover, let us note that an absolute value of the relative gain error less than 6% is obtained for quadrature errors less than 3.2° irrespective of the imposed phase shifts $\Phi_{\text{th}} \in [-90° \cdots 90°]$. From Fig. 4*b*, it can be concluded that the absolute phase error is maximum when Φ_{th} equals $\pm 45°$ and zero when Φ_{th} equals 0°, $-90°$ and $+90°$ irrespective of ε_q. Furthermore, we can say that an absolute phase error less than 3° is obtained for quadrature errors less than 3.2° irrespective of the imposed phase shifts $\Phi_{\text{th}} \in [-90° \cdots 90°]$.

Since [32], vector modulators with less than 3° phase error (ε_q) and 0.5 dB (6%) magnitude error (k_A) can be designed especially for image rejection. Therefore according to the

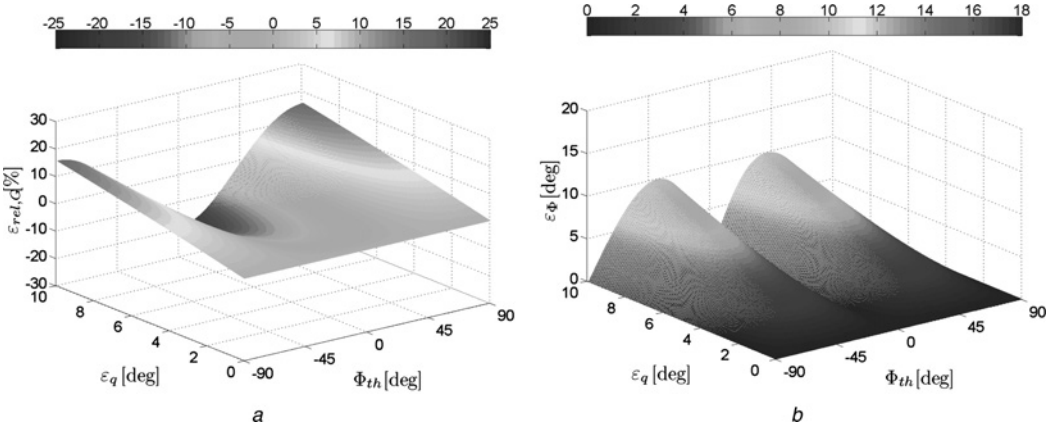

Figure 4 *Influence of the quadrature error ε_q*

a Relative gain error $\varepsilon_{\text{rel},G}$
b Absolute phase shift error ε_Φ

IET Microw. Antennas Propag., 2011, Vol. 5, Iss. 2, pp. 245–254
doi: 10.1049/iet-map.2010.0005

proposed theoretical study, the vector modulator-based active phase shifter can achieve the limit of 5° absolute phase error (ε_{Φ}) and 0.5 dB (6%) relative gain error ($\varepsilon_{\mathrm{rel},G}$) which are reasonable demands for the targeted application [33].

2.2 System analysis of the active phase shifter architecture

Another source of errors is the accuracy of the DC command voltages $V_{\mathrm{I}m}$ and V_{Q_m}, $m = 1 \cdots N$, provided by a drive circuit which is a numerical one. For instance, the quantisation noise and the clock signal will disturb the command voltages. Average Gaussian white noise can model this perturbation. In order to study the impact of this noise on the communication system performances, simulations were done using the architecture shown in Fig. 5.

For these simulations, the case of a four 'patch' antenna array is considered. A constant phase gradient $\Delta\Phi = \Phi_{m+1} - \Phi_m = 100^\circ$ is imposed and a quadrature phase-shift keying modulation (QPSK) is chosen for its high sensitivity to phase noise. Symbol rate is set to 11 Mbps with a carrier frequency $f_0 = 2.4$ GHz. Under these conditions, Fig. 6*a* shows the constellation generated by each vector modulator driven by noisy DC commands when the root mean square (RMS) noise voltage is set to $150(\mu\mathrm{V}/\sqrt{\mathrm{Hz}})$. At the receiver, a dual architecture allows one to recover the original constellation. The results are presented in Fig. 6*b*. As can be seen in this figure, the transmission quality is degraded.

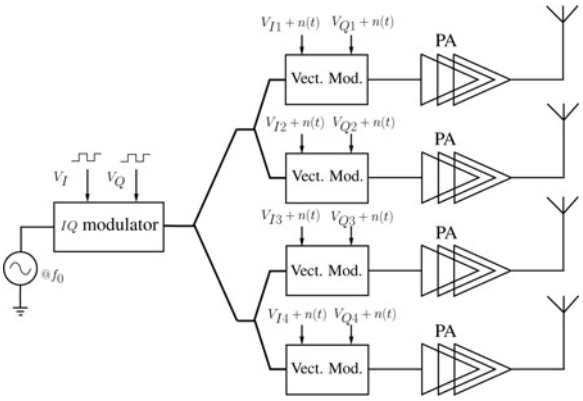

Figure 5 *System architecture using vector modulators*

In order to quantify this degradation, the variation of the error vector magnitude (EVM) against the RMS noise voltages is simulated. First of all, Fig. 7*a* shows the impact of the RMS noise voltage on each antenna for a main lobe steering angles $\theta_{\mathrm{M.L.}} \simeq 30^\circ$ (corresponding to $\Delta\Phi = 100^\circ$). As can be seen from this figure, the EVM is independent of the DC command voltages $V_{\mathrm{I}m}$ and V_{Q_m}.

Fig. 7*b* shows the EVM evolution always against noise voltages but for different main lobe steering angles $\theta_{\mathrm{M.L.}}$. It can be concluded that the EVM hardly changes with the required transmission direction because of the low signal bandwidth to carrier frequency ratio. Nevertheless, for a noise voltage higher than $2\,(\mathrm{mV}/\sqrt{\mathrm{Hz}})$, we can observe a slight difference between each curve. This is because of the fact that, in this case, the command voltage to noise voltage ratio, defined in [34] as $C_{\min}/N$ (with $C_{\min}$ the minimum value of the DC command voltages and N the noise voltage), becomes significant and implies degradations and dispersions on the overall system performances. Indeed, let us remind that the main lobe steering angle $\theta_{\mathrm{M.L.}}$ depends on the DC command voltages applied on each vector modulator. Thus, the $C_{\min}$ value changes with the required main lobe steering angle $\theta_{\mathrm{M.L.}}$. In these conditions, for a given noise voltage higher than $2\,(\mathrm{mV}/\sqrt{\mathrm{Hz}})$, the $C_{\min}/N$ value also changes with the required main lobe steering angle as well as the EVM [34]. However, in normal conditions of use, the noise voltage

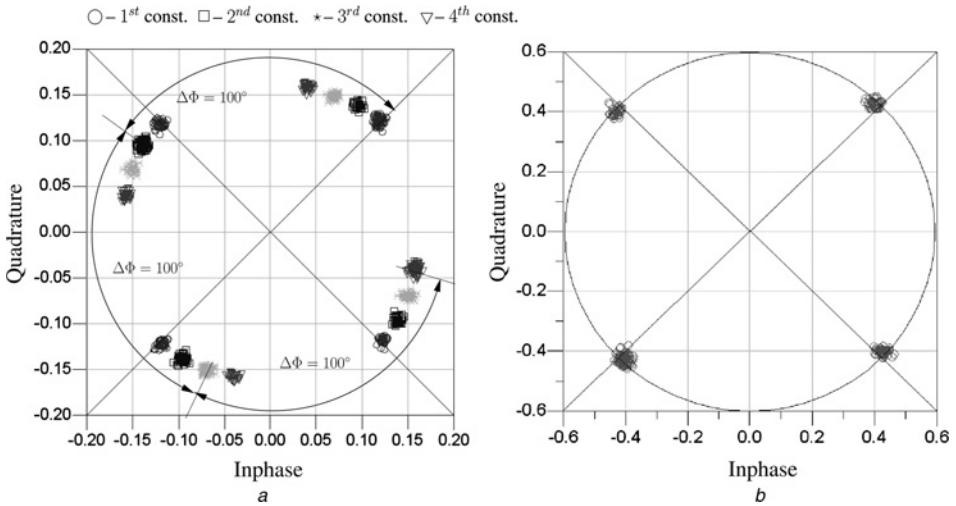

Figure 6 *Emitted and received signal constellation simulated EVM: 2.8%*

a Emitted signal constellation
b Received signal constellation

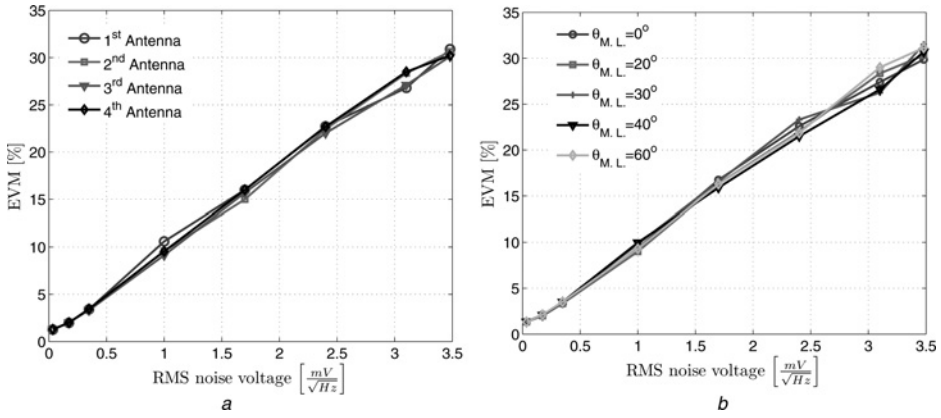

Figure 7 *Influence of the noise voltage: the EVM against RMS noise voltage*

a On each antenna
b For various depointing angles

level is close to the quantisation noise and thus less than 2 (mV/$\sqrt{\text{Hz}}$). Anyway, these system simulations prove the necessity to take into account the noise which can be added to the DC command voltages. Indeed, this noise directly implies transmission perturbations. For example, command noise voltages less than 0.8 (mV/$\sqrt{\text{Hz}}$) are required in order to achieve an EVM level lower than 8.5%.

So, by taking into account all these constraints, the design of a prototype including the antenna array becomes possible.

3 Measurement results

A prototype with four 'patch' antennas using discrete components was implemented on a G-10/FR-4 printed circuit board with $\varepsilon_r = 4.6$; $\tan\delta = 10^{-2}$ and conductive layer height $h = 0.35$ μm. As can be seen in Fig. 8*a*, the prototype is made of two parts:

1. a 'drive circuit' built around an 8-bit RISC micro controller. This micro controller converts the amplitudes and phases levels given by a laptop via a USB connection in bit sequences. An 8-bit serial DAC and an S/H + MUX architecture generate the corresponding V_I and V_Q DC voltages applied to the vector modulator inputs.

2. an 'RF circuit' made of four elementary RF blocks, a distribution tree and four 'patch' antennas. An AD 8394 vector modulator and an output amplifier working in the linear region represent the active parts of the elementary RF blocks. Input and output 1:1 transmission line transformers allow the single to differential mode transitions.

First of all, S parameter measurements of the elementary RF blocks without antennas were performed at 2.4 GHz. As can be seen in Fig. 9*a*, the measured value of the input reflection coefficient S_{11} is less than −15 dB, whereas the value of S_{22} is close to −8.5 dB mainly because of the S_{22} parameter of the output amplifier. Furthermore, let us note that these two parameters are identical for all RF blocks.

Concerning the transmission parameter S_{21} of each elementary RF block, magnitudes and phase shifts goals were defined and compared with measurements (Fig. 9*b*).

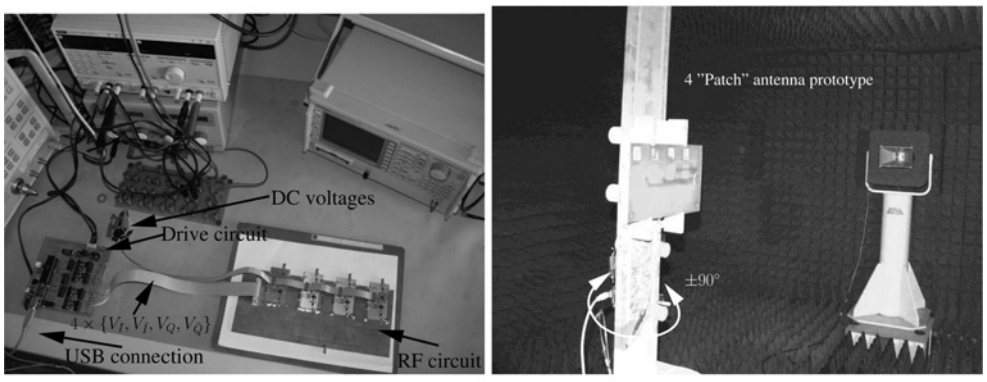

Figure 8 *Setup for the radiation pattern measurements*

a Prototype
b Anechoic chamber

IET Microw. Antennas Propag., 2011, Vol. 5, Iss. 2, pp. 245–254
doi: 10.1049/iet-map.2010.0005

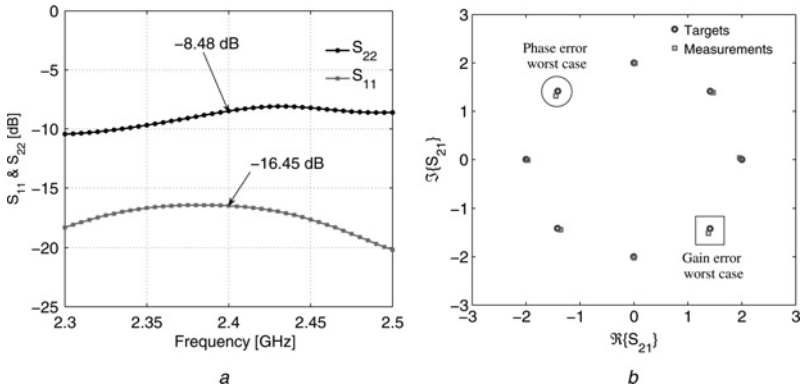

Figure 9 *S parameters of an elementary RF block*

a S_{11} and S_{22}
b S_{21} @ 2.4 GHz for imposed phase shifts

In these conditions, the maximum gain error $\varepsilon_{\text{rel},G}$ is close to 2.5% and the absolute value of the phase shift error ε_{Φ} is less than 3° as shown in Fig. 10. Those measured values are below the limits of 6% and 5° mentioned in Section 2. In order to complete this characterisation, the measured 1 dB output compression point is −6 dBm.

Now, in order to verify the ability of the system to perform beamforming, let us consider an array of $N = 4$ identical equidistant antennas ($d = \lambda_0/2$, $f_0 = 2.4$ GHz) and let us suppose that the direction of the desired signal is $\theta_u = 30°$ and the direction of the interference signal is $\theta_i = -15°$. The θ angles are measured in the $y0z$-plane starting from the $0y$-axis. By using the least mean squares based beamforming algorithm given in [35], the obtained amplitudes and phases, computed as the modules and the phases of the complex weights w (Fig. 1), are given in Table 1. Under these conditions, the simulated radiation pattern (using Agilent Momentum software) is presented in Fig. 11. It can be seen that if the complex coefficients given in Table 1 are assured, the maximum gain is presented in the signal of interest direction: $\theta_u = 30°$ and a null is placed in the interference signal direction: $\theta_i = -15°$.

In these conditions, measurements in an anechoic chamber (Fig. 8*b*) were performed. V_I an V_Q DC voltages

Table 1 Amplitudes and phases necessary for four antennas in the $\theta_u = 30°$ and $\theta_i = -15°$ scenario

A_m	0.21	0.29	0.29	0.21
ϕ_m	10.51°	−110.4°	176.3°	55.3°

corresponding to the amplitudes and phases given in Table 1 were first applied. An RF signal @ 2.4 GHz and −10 dBm power provided by a 'Wiltron 360' 40 GHz network analyser was also applied to the prototype.

Fig. 12 shows the theoretical and measured radiation patterns. Theoretical radiation patterns were calculated using Matlab software by multiplying the radiation pattern of one patch antenna with the theoretical array factor. As expected, the measured radiation pattern presents a maximum gain in the 31° direction and a null in the −15° direction. Other radiation pattern measurements at five different main lobe directions are presented in Fig. 13. Let us note that the radiation pattern in Fig. 13*d* does not respect the imposed $\theta_{\text{M.L.}}$ direction because the visible region of a 'patch' antenna is inside $[-45° \cdots +45°]$ interval.

Differences between the theoretical and the measured radiation patterns can be remarked on Figs. 12 and 13. These differences, especially between the measured and

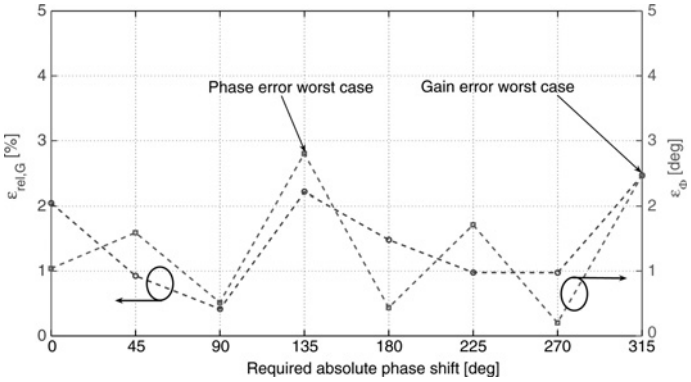

Figure 10 *Measured relative gain error and absolute phase error of an RF block*

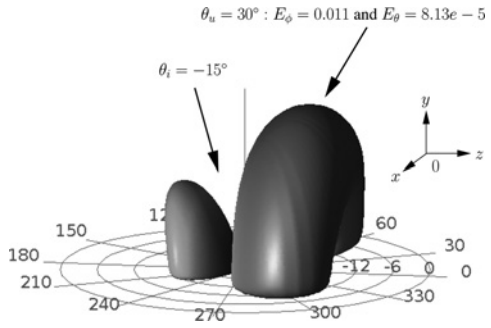

Figure 11 *Three-dimensional simulated radiation pattern of four 'patch' antennas*

theoretical side lobes, are mainly because of the finite ground plane of the antennas. As can be seen in Fig. 1, the antennas are placed near the edges of the prototype. This vicinity will alter the ideal radiation pattern of a patch antenna. Another cause of the differences between the measured and theoretical radiation patterns is the electromagnetic mutual coupling between the patch antennas. This coupling is not modelled when the theoretical radiation patterns are calculated. Moreover, the differences between the two radiation patterns are because of the fact that the four patch antennas do not have exactly the same behaviour. Only one of four radiation patterns was considered when the theoretical radiation pattern was calculated.

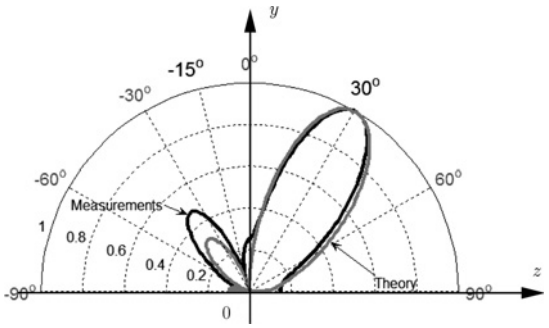

Figure 12 *Measured and theoretical normalised radiation patterns: expected $\theta_u = 30^\circ$ and $\theta_i = -15^\circ$*

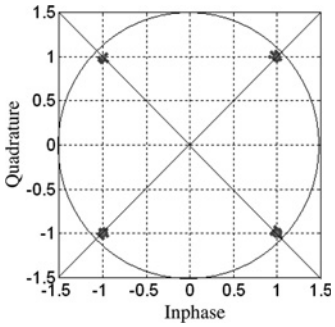

Figure 14 *Measured received constellation in the case of $\theta_{M.L.} = 30^\circ$*

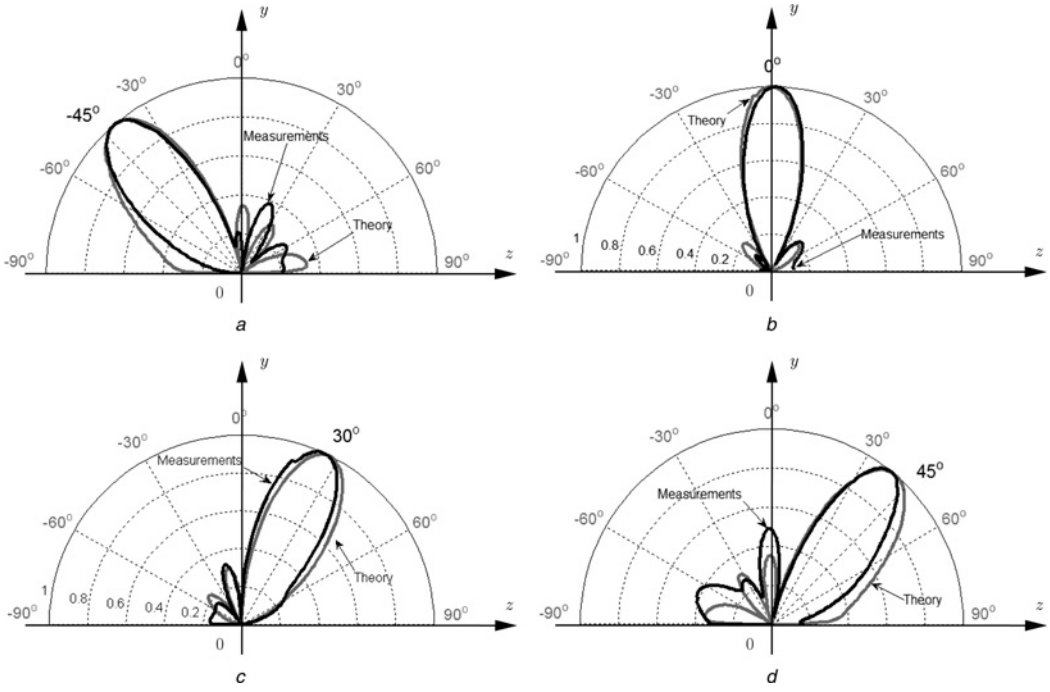

Figure 13 *Measured and theoretical normalised radiation patterns without beamforming*

a Main lobe pointing towards $\theta_{M.L.} = -45^\circ$
b Main lobe pointing towards $\theta_{M.L.} = 0^\circ$
c Main lobe pointing towards $\theta_{M.L.} = 30^\circ$
d Main lobe pointing towards $\theta_{M.L.} = 45^\circ$

IET Microw. Antennas Propag., 2011, Vol. 5, Iss. 2, pp. 245–254

doi: 10.1049/iet-map.2010.0005

Having demonstrated the abilities to control the shape of the radiation pattern, EVM measurements were performed by applying digital modulated signals on this system. Fig. 14 shows an example of the received constellation measured in the anechoic chamber, for a QPSK modulation with a carrier frequency $f_0 = 2.4$ GHz and a 7 MHz bandwidth. The depointing angle was set to $\theta_{M.L.} = 30°$. The mean EVM measured during 1000 bit periods is 5.5% mainly because of noisy DC command voltages V_{I_m} and V_{Q_m}, $\forall m \in [1 \cdots 4]$. Once again, this experimental result proves the necessity to take into account the noise added on the DC command voltages.

4 Conclusion

A 2.4 GHz antenna array using vector modulators working as active phase shifters was presented in this paper. Electronic beamforming using vector modulators presents a lot of advantages, in particular an improved signal to noise ratio (SNR) during transmission, and a better use of the transmitters' output power. In this paper, a theoretical analysis is first performed in order to quantify the impact of vector modulator I/Q mismatch on the synthesised amplitudes and phases of the signals applied on each elementary antenna. System analysis is also performed in order to study the impact of noisy DC command voltages on the system performances. By taking into account these non-ideal behaviours, a 2.4 GHz prototype with four 'patch' antennas was implemented and characterised in an anechoic chamber. The measured radiation patterns are consistent with the theoretical results. Furthermore, the measured output signal constellation, for a QPSK modulation with a carrier frequency $f_0 = 2.4$ GHz and a 7 MHz bandwidth, is also presented and the mean EVM measured is 5.5%.

5 Acknowledgments

The authors thank the 'Poitou-Charentes' region council for their financial support of this work. They also thank M. David Carsenat and M. Cyril Decroze from XLIM Research Institute, Limoges, France, for helpful discussions and their contribution to the radiation pattern measurements.

6 References

[1] SIMONS J., IVASHINA M., BIJ DE VAATE J.G., RODDIS N.: 'Beamformer system model of focal plane arrays in deep dish radio telescopes'. European Radar Conf. 2005, EURAD 2005, 6–7 October 2005, pp. 355–358

[2] LILJA P., SAARNISAARI H.: 'Robust adaptive beamforming in software defined radio with adaptive diagonal loading'. IEEE Military Communications Conf., 2005, MILCOM 2005, 17–20 October 2005, vol. 4, pp. 2596–2601

[3] NATARAJAN A., KOMIJANI A., HAJIMIRI A.: 'A 24 GHz phased-array transmitter in 0.18 μm CMOS'. Proc. 42nd Design Automation Conf., 2005, pp. 551–552

[4] FABRIZIO G., COLONE F., LOMBARDO P., FARINA A.: 'Adaptive beamforming for high- frequency over-the-horizon passive radar', *IET Radar Sonar Navig.*, 2009, **3**, (4), pp. 384–405

[5] SARKAR T.K., WIEKS M.C., SALAZAR-PALMA M., BONNEAU R.J.: 'Smart Antennas' (John Wiley & Sons, Inc., 2003)

[6] BALANIS C.A., IOANNIDES P.I.: 'Introduction to Smart Antennas' (Morgan & Claypool, 2007)

[7] HANSEN R.C.: 'Phased Array Antennas' (Wiley-Interscience, 2001)

[8] GODARA L.C.: 'Application of antenna arrays to mobile communications', part I: performance improvement, feasibility and system considerations', *IEEE Proc.*, 1997, **85**, (8), pp. 212–230

[9] GODARA L.C.: 'Application of antenna arrays to mobile communications, part II: beam-forming and direction-of-arrival considerations', *IEEE Proc.*, 1997, **85**, (8), pp. 212–230

[10] LYNCH J.J., YORK R. A.: 'Synchronization of oscillators coupled through narrowband networks', *IEEE Trans. Microw. Theory Tech.*, 2001, **49**, (2), pp. 237–249

[11] GUAN X., HASHEMI H., HAJIMIRI A.: 'A fully integrated 24-GHz eight-element phase-darray receiver in silicon', *IEEE J. Solid-State Circuits*, 2004, **39**, (12), pp. 2311–2320

[12] NATARAJAN A., KOMIJANI A., HAJIMIRI A.: 'A fully integrated 24-GHz phased-array transmitter in CMOS', *IEEE J. Solid-State Circuits*, 2005, **40**, (12), pp. 2502–2514

[13] LIAO P., YORK R.A.: 'A new phase-shifterless beam-scanning technique using arrays of coupled oscillators', *IEEE Trans. Microw. Theory Tech.*, 1993, **41**, (10), pp. 1810–1815

[14] FUCHS H.-H., NUSSLER D.: 'Design of Rotman lens for beamsteering of 94 GHz antenna array', *Electron. Lett.*, 1999, **35**, (11), pp. 854–855

[15] TSENG C.-H., CHEN C.-J., CHU T.-H.: 'A low-cost 60-GHz switched-beam patch antenna array with butler matrix network', *IEEE Antennas Wirel. Propag. Lett.*, 2008, **7**, pp. 432–435

[16] YORK R.A., POPOVIC Z.B.: 'Active and quasi-optical arrays for solid-state power combining' (John Wiley & Sons, Inc., 1997)

[17] YORK R.A., ITOH T.: 'Injection and phase-locking techniques for beam control', *IEEE Trans. Microw. Theory Tech.*, 1998, **46**, (11), pp. 1920–1929

[18] HEATH T.: 'Simultaneous beam steering and null formation with coupled, nonlinear oscillator arrays', *IEEE Trans. Antennas Propag.*, 2005, **53**, (6), pp. 2031–2035

[19] ELLINGER F., BÄCHTOLD W.: 'Novel principle for vector modulator-based phase shifters operating with only one control voltage', *IEEE J. Solid-State Circuits*, 2002, **37**, (37), pp. 1256–1259

[20] PARAMESH J., BISHOP R., SOUMYANATH K., ALLSTOT D.J.: 'A four-antenna receiver in 90-nm CMOS for beamforming and spatial diversity', *IEEE J. Solid-State Circuits*, 2005, **40**, (12), pp. 2515–2524

[21] GUEORGUIEV S., LINDFORS S., LARSEN T.: 'A 5.2 GHz CMOS I/Q Modulator with integrated phase shifter for beamforming', *IEEE J. Solid-State Circuits*, 2007, **42**, (9), pp. 1953–1962

[22] KOH K.-J., REBEIZ G.M.: '0.13-μm CMOS phase shifters for X-, Ku-, and K-band phased arrays', *IEEE J. Solid-State Circuits*, 2007, **42**, (11), pp. 2535–2546

[23] AZARO R., IORIATTI L., MARTINELLI M., BENEDETTI M., MASSA A.: 'An experimental realization of a fully adaptive smart antenna', *Microw. Opt. Technol. Lett.*, 2008, **50**, (6), pp. 1715–1716

[24] BENEDETTI M., AZARO R., MASSA A.: 'Experimental validation of fully-adaptative smart antenna prototype', *Electron. Lett.*, 2008, **44**, (11), pp. 661–662

[25] BENEDETTI M., OLIVERI G., ROCCA P., MASSA A.: 'A fully-adaptive smart antenna prototype: ideal model and experimental validation in complex interference scenarios', *Prog. Electromagn. Res.*, 2009, **96**, pp. 173–191

[26] CHANDRAN S.: 'Adaptative antenna arrays. Trends and applications' (Springer-Verlag, 2004)

[27] PLAPOUS C., CHENG J., TAILLEFER E., HIRATA A., OHIRA T.: 'Reactance domain MUSIC algorithm for ESPAR antennas'. 33rd European Microwave Conf., October 2003, pp. 793–796

[28] HAUPT R.L., SOUTHALL H.: 'Experimental adaptive nulling with a genetic algorithm', *Microw. J.*, 1999, **42**, pp. 78–89

[29] WEILE D.S., MICHIELSSEN E.: 'The control of adaptive antenna arrays with genetic algorithms using dominance and diploidy', *IEEE Trans. Antenna Propag.*, 2001, **49**, pp. 1424–1433

[30] BENEDETTI M., AZARO R., MASSA A.: 'Memory enhanced PSO-based optimization approach for smart antennas control in complex interference scenarios', *IEEE Trans. Antennas Propag.*, 2008, **56**, (7), pp. 1939–1947

[31] HUTU F., CORDEAU D., PAILLOT J.-M.: 'A 2.4 GHz active phase shifter architecture for smart antennas control'. IEEE MTT-S Int. Microwave Symp., 2009, pp. 821–824

[32] STEYAERT M., ROOVERS R.: 'A 1 GHz single-chip quadrature modulator', *IEEE J. Solid-State Circuits*, 1992, **27**, (8), pp. 1194–1197

[33] ELLINGER F., LOTT U., BACHTOLD W.: 'An antenna diversity MMIC vector modulator for HIPERLAN with low power consumption and calibration capability', *IEEE Trans. Microw. Theory Tech.*, 2001, **49**, (5), pp. 964–969

[34] TOHMÉ N., PAILLOT J.-M., CORDEAU D., CAUET S., MAHÉ Y., RIBARDIÈRE P.: 'A 2.4 GHz 1-dimensional array antenna driven by vector modulators'. IEEE MTT-S Int. Microwave Symp., 2008, pp. 803–806

[35] FROST III O.L.: 'An algorithm for linearly constrained adaptive array processing', *Proc. IEEE*, 1972, **60**, (8), pp. 926–935

doi: 10.1049/iet-map.2010.0005